Arch Bridges
ARCH´04
P. Roca and E. Oñate (Eds)

THE BEHAVIOUR OF OPEN SPANDREL MASONRY ARCH BRIDGES

C. Melbourne*, H.Tao†

*School of Computing, Science and Engineering, Newton Building, University of Salford, M5 4WT
email: c.melbourne@salford.ac.uk
† Kvaerner E&C UK Ltd, Ashmore House, Richardson Road, Stockton-on-Tees, TS18 3RE

Keywords: Masonry, arch, open-spandrel, FE Modelling

Abstract. *Open spandrel masonry arch bridges comprise a main arch which supports subsidiary arches spanning in the same direction. Such bridges have been used for well over 1000 years.*
The paper reports on the behaviour of one of a series of large scale laboratory tests and two methods of FE modelling. It is shown that failure occurred by the formation of both local and global mechanisms. Additionally, it is reported that both smeared and discrete FE moulds give reasonably good correlations with the test model, although they were quite sensitive to the tensile strength of the masonry. The Fe moulds were less sensitive to Young's modulus and compressive strength when predicting ultimate bad capacity.

1 INTRODUCTION

Masonry arch bridges have enjoyed a long and respected history in both Western and Eastern societies. Their roots lie in antiquity and although their popularity for new construction has faltered in recent years in the West, no such recession is evident in the East where masonry arch bridge construction has continued uninterruptedly in modern times.

Open spandrel masonry arch bridges comprise a main arch which supports subsidiary arches spanning in the same direction. Compared with filled spandrel masonry arch bridges, the former has some apparent advantages over the latter, such as reduction of overall dead-weight, space to accommodate flood water etc. Such bridges have been widely used since as early as 600 AD in China and since the seventeenth century in Europe.

2 MODEL ARCH BRIDGES TESTS

A total of five model tests on brickwork arches were constructed. The dimensions of each of the models are given in Table 1 and the material properties in Table 2. A full report of all tests can be found elsewhere (Tao, 2003). This paper will concentrate on just one of the tests, OSMA 3. (Table1, Figure 1)

For all the models arches, the main arches and spandrel arches were segmental. Header bond was used throughout to eliminate the possibility of ring separation. It may be noted that the same bricklayer was used for the construction of all arch models and brickwork prisms to maintain consistency.

	OSMA1	OSMA2	OSMA3	OSMA4	OSMA5
M. A.					
Span (mm)	-	3,000	5,000	5,000	5,000
Rise (mm)	-	750	1,250	1,250	1,250
γ	-	4	4	4	4
Thickness (mm)	-	178	215	215	215
Bricks	-	H. S. R	E. C. A	E. C. A	E. C. A
S. A.					
Span (mm)	250	250	550	-	550
Rise (mm)	50	50	110	-	110
γ	5	5	5	-	5
Thickness (mm)	54	54	100	-	100
Bricks	H. S. R	H. S. R	E. C. A	-	E. C. A
S. P.					
Width (mm)	114	114	178	-	178
Height (mm)	393, 162	393, 162	550	-	550
Bricks	H. S. R	H. S. R	H. S. R	-	H. S. R
Arch Width (mm)	500	500	1,000	1,000	1,000

Fill	-	-	-	-	Mortar
Self Weight (kg)	100	700	4,500	2,950	5,300
Max. Load (kN)	13.00	13.50	23.50	12.50	32.50
Loading Position When Collapse	1/4L of End S.A. On LHS	Top of The Short Pier	Top of The Arch Seat	Quarter-Span	Top of The Arch Seat

Note:
(1) M. A. - main arch; S. A. - spandrel arch; and S. P. - spandrel pier; γ - Span/Rise
(2) E. C. A - Class A Engineering Brick; H. S. R - half scale Raewell brick;
(3) Density: - 2.30 t/m^3 for E. C. Brickwork; 1.80 t/m^3 for H. S. R. brickwork; 1.54 t/m^3 for mortar.

Dimensions of the Model Arches and Loading Capacities Table 1

During the model tests, no movement of the abutments of the main arches was recorded.

2.1 Five metre Span OSMA 3 test

A total of seven elastic (ET) tests were carried out for the model. The loading locations and the loads applied are shown as in Fig. 1 and Table 2, respectively. Fine cracks developed within the end spandrel arches in the vicinity of the loads when they were applied at the crowns of spandrel arch 1 (SA1) and spandrel arch 4 (SA4).

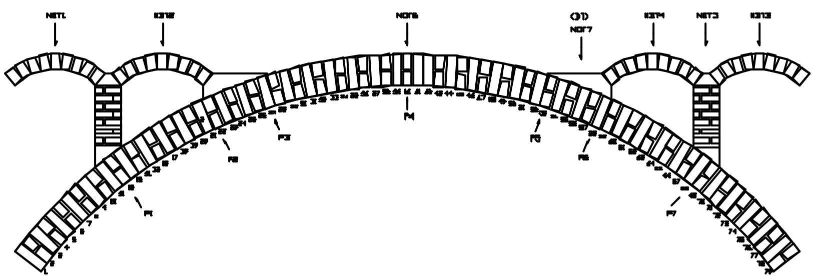

Fig. 1 Model Tests of OSMA3

ET	1	2	3	4	5	6	7	DT
Max Load (kN)	5.0	18.0	5.0	9.0	10.0	20.0	18.0	23.5

Summary of ET and DT Tests of OSMA3 Table 2

The model failed when monotonic loading to 23.5 kN was applied at the arch seat on the right hand side. Fig.3 shows the typical relationships between the radial deflections along the intrados of the main arch and the applied loads with loading at top of the arch seat (DT).

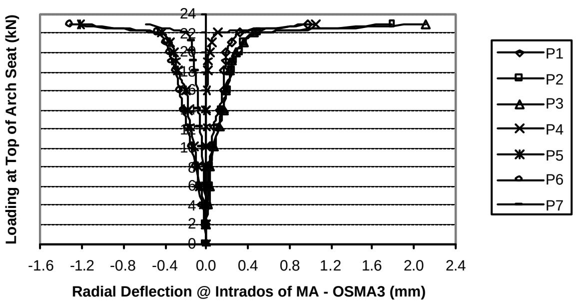

Fig. 2 Load Deflection Curves of OSMA3 with Loading at ¼ Span of MA

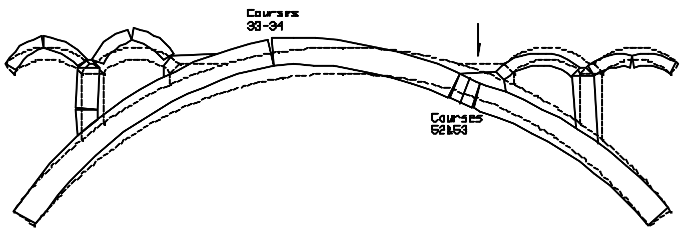

Fig.3 Global and Local Failure Modes of OSMA3

Global and local failure modes of the model were observed (Figure 3). For the main arch, the failure was due to the formation of four hinges. The first set of obvious cracks occurred between the brick courses 51 and 52 and between 33 and 34. The piers failed at the sections when their flexural tensile strengths were exceeded. For the spandrel piers, the local failure mechanism was due to the movement/rotation of the abutments/supports.

3 FINITE ELEMENT MODELS

Brickwork is a complex, composite material comprising bricks bonded with mortar. The properties of the components, the conditions of the interface bonds and the patterns in which the bricks are assembled all affect the behaviour of the brickwork. Three different FE models were developed using ANSYS 5.3 i.e. smeared, discrete and mixed idealisations. Only the first two methods are dealt with in the paper

Through preliminary modelling studies, it was concluded that the element, SOLID 65, of ANSYS 5.3 could be used as it is designed to model cracking tension, crushing in compression and other plastic behaviour of a brittle material. The material modelled was assumed to be a homogeneous continuum, and virtually isotopic. For simplicity and computational efficiency, only one layer of elements was generated along the width of the model, considering that it was a 2D model i.e. a plane stress condition. The material properties used in the smeared model are presented in Table 3, which is based, where possible, upon material tests.

Figure 4 shows a comparison between the model test and the FE model for the radial deflection-load. Figure 5 shows the simulated cracking sequence using the smeared model, which can be compared with the model arch collapse in figure 3.

Poisson's Ratio	0.20
Shear Transfer Coefficient For Open Cracks (β1)	0.01
Shear Transfer Coefficient For Close Cracks (β2)	0.10
For Main Arch and Spandrel Arches	
Density	2300 (kg/m^3)
Young's Modulus	10000 (N/mm^2)
Uniaxial Crushing Strength (σc)	18.00 (N/mm^2)
Uniaxial Tensile Cracking Strength (σt)	0.30 (N/mm^2)
For Spandrel Piers	
Density	1800 (kg/m^3)
Young's Modulus	3500 (N/mm^2)
Uniaxial Crushing Strength (σc)	7.50 (N/mm^2)
Uniaxial Tensile Cracking Strength (σt)	0.25 (N/mm^2)

Material Properties for the Analysis of SM OSMA3 Table 3

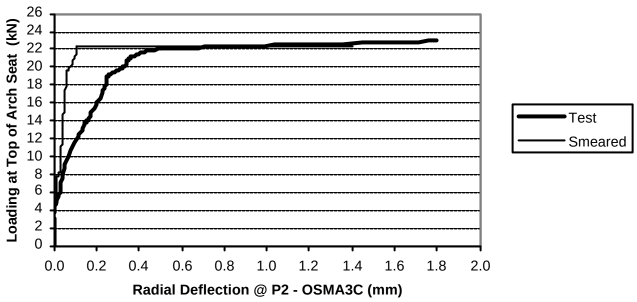

Fig. 4 Load-Deflection curves at P2 OSMA3 Using Smeared Model

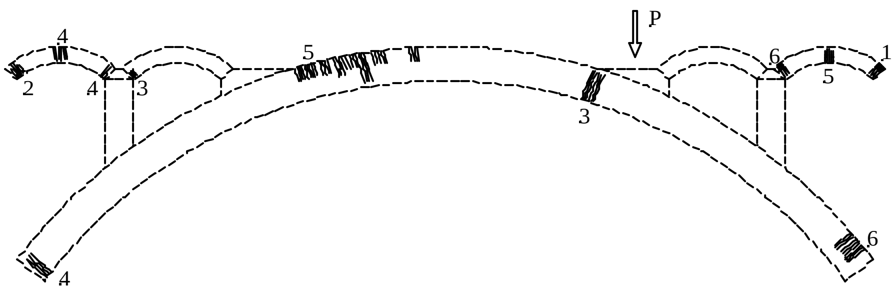

Fig. 5 Simulated Cracking Sequences of OSMA3 Using Smeared Model

The material properties for the discrete FE model are given in Table 4. The simulated mode of failure and sequence of hinge development are shown in Figure 7 and Table 5, respectively, and a typical load-deflection curve is shown in Figure 8.

For Main Arch and Spandrel Arches	
Density	2300 (kg/m^3)
Poisson's Ratio	0.20
Young's Modulus	10000 (N/mm^2)
For Spandrel Piers	
Density	1800 (kg/m^3)
Poisson Ratio	0.20
Young's Modulus	3500 (N/mm^2)
For CONTAC48	
Coefficient Of Friction	0.80
Normal Stiffness	10000 (N/mm)
Tangential Stiffness	1000 (N/mm)
For COMBIN40 Elements In Radial Direction	
Bond Strength	0.0001 (N/mm^2)
Stiffness Of Master Spring	0.01 (N/mm)
Stiffness Of Slave Spring	0.001 (N/mm)
For COMBIN40 Elements In Tangential Direction	
Bond Strength	0.0001 (N/mm^2)
Stiffness Of Master Spring	0.01 (N/mm)
Stiffness Of Slave Spring	0.001 (N/mm)
Locations Of Potential Failure Sections	
To The Springing Of Main Arch	30 (mm)
To The Bottom Of Spandrel Piers	90 (mm)
To The Springing Of End Spandrel Arches	20 (mm)
To The Crown Of Main Arch (Unloaded Side)	600 (mm)

Material Properties for the Analysis of DM OSMA3 Table 4

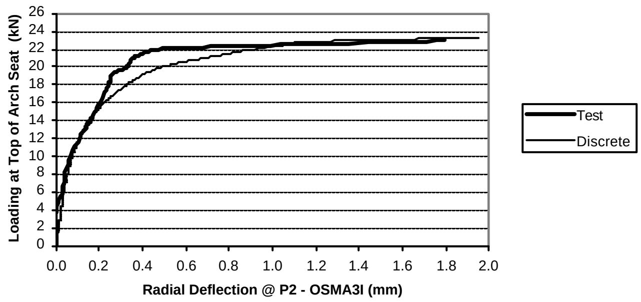

Fig.8 Load-Deflection Curves at P2 of OSMA3 Using Discrete Model

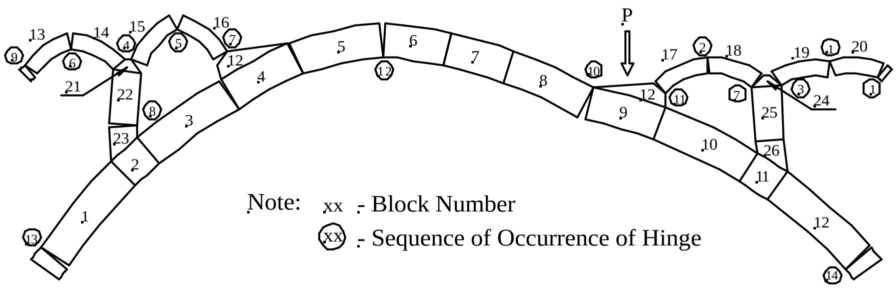

Fig.7 Simulated Mode of Failure of OSMA3 using Discrete Model

Hinge No	**Loads (kN)**	**Locations**
1	Self-weight	SA4 (Crown & Right End)
2	0.8	SA3 (Crown)
3	4.1	SA4 (Left End)
4	6.9	SA2 (Left End)
5	9.1	SA2 (Crown)
6	9.6	SA1 (Crown)
7	10.2	SA2 & SA3 (Left Ends)
8	10.4	Pier1
9	11	SA1 (Left End)
10	19.9	MA (Under load)
11	21.6	SA3 (Left End)
12	22.8	MA (Near Crown)
13	23.1	MA (Left End)
14	23.6	MA (Right End)

Sequence of Hinge Development and Corresponding Load Table 5

4 DISCUSSION

The behaviour of open spandrel brickwork arches was studied through as series of model arch tests and finite element simulations. A total of five brickwork model arches were constructed and tested, only one of which is reported herein.

Most of the properties used in the FE models were obtained through various material tests. The values of other parameters used in the FE model were justified through sensitivity studies (Tao, 2003). Both the observed and recorded behaviour of the model arches during the tests could be reproduced by the smeared and/or discrete models. Reasonably good correlations were achieved in terms of the ultimate loads, the pattern of cracks or hinges and load-displacement responses between the test results and the FE models

For the smeared models, the required materials-related parameters include Poisson's ratio, density, and Young's modulus; and the required elements-related parameters include shear transfer coefficients for open and closed cracks; uniaxial crushing strength; and uniaxial tensile cracking strength. The change in the value of Poisson's ratio has little effects on the behaviour of arches, and a value between 0.15 and 0.3 may be assumed. If an average of the Young's moduli obtained from the standard prism tests is used in FE analyses of a masonry arch, stiffer responses are likely to be predicted. The Young's modulus used in the FE analyses has little effects on the ultimate loads predicted. Thus, it can be determined with certain confidence as far as the determination of the load capacity of a masonry arch is concerned. Any value between 0 and 1 inclusive for the shear transfer coefficient for closed cracks hardly have any effect on the behaviour of arches, and shear transfer coefficient for open cracks did have some effect on the development of cracks and ultimate loads if values over 0.7 were used. However, considering that brickwork arches generally fail due to the formation of hinges and shear strengths between mortar joints are relatively low, small values between 0.01 and 0.1 may be used for shear transfer coefficients for closed and open cracks. The uniaxial crushing strength of brickwork masonry can be obtained through prism tests. As the stresses within masonry arches through loading history are generally less than the uniaxial crushing strength, the accuracy of the uniaxial crushing strength obtained from prism tests may not be critical. The last parameter required is the uniaxial tensile strength of masonry, which may need special attention. The success of the analyses using the smeared model largely depends on the tensile strength of brickwork masonry. The tensile strength of brickwork masonry may be obtained through the tensile tests of brickwork prisms. Otherwise, a value between 0.28 and 0.30 N/mm2 was normally sufficient to realistically simulate the behaviour of brickwork masonry arches.

For the discrete models, the required materials-related parameters are the same as those for the smeared models, i.e., Poisson's ratio, density, and Young's modulus. The same principles as those discussed for the smeared models may be used to determine their values. The required elements-related parameters mainly include coefficient of friction, normal stiffness and tangential stiffness. The coefficient of friction may be obtained from shear tests of two-course brickwork prism. However, since the results from tensile tests are likely to be scattered, a representative value may not be readily determined. It has been found that any value over 0.4 (note that the average of test results are normally well over 0.4) could normally ensure the success of the analyses.

The normal stiffness of contact elements may be assumed the same as the Young's modulus obtained from the prism tests of the corresponding model arch, and the tangential stiffness may be assumed as 1/10 or 1/100 of the normal stiffness.

5 CONCLUSIONS

The following conclusions may be drawn from the laboratory test and FE modelling of open spandrel brick masonry arches:

- Failure occurred by the formations of both local and global hinged mechanisms. There were four hinges in the main arch and sufficient hinges in the spandrel arches to create a local mechanism (i.e. in this case seven hinges)
- The location of the third hinge within the main arch moved towards the crown due to the interaction between the spandrel structure and the main arch.
- Both smeared and discrete FE models give reasonably good correlations with the test models, although they were quite sensitive to tensile strength the models were less sensitive to Young's modulus and compressive strength when predicting ultimate load capacity.

Acknowledgements

The authors wish to acknowledge the support of the University of Salford and Marshall Products Ltd

Reference

[i] H. Tao *The Behaviour of Open Spandrel Brickwork Masonry Arch Bridges* (2003), PhD Thesis, University of Salford